# THE DYNAMIC WHEEL-RAIL CONTACT STRESSES FOR WAGON ON VARIOUS TRACKS

**Fujie Xia*, Colin Cole# and Peter Wolfs#**

* Rail CRE, Faculty of Sciences, Engineering and Health
Central Queensland University, Rockhampton, QLD 4702, Australia
# Rail CRE, Faculty of Sciences, Engineering and Health
Central Queensland University, Rockhampton, QLD 4702, Australia

f.xia@cqu.edu.au

## ABSTRACT

The maximal stress and tangential surface forces at the wheel rail contact elliptic area are affected by the wheel rail contact dynamic load and creepages. Dynamic wheel load is related to the wagon dynamic system, track and wheel rail interaction. Creepages are related to the motion of wheelset and wheel rail contact parameters. The paper presents an analysis of the effects of creepages on wheel rail contact forces. A complete Australia wagon with three-piece bogies was modelled and various tracks were selected for the simulation of dynamic wheel rail contact stresses. The results show that the maximal normal wheel rail contact stresses is under $1600Mpa$ in a range of conditions typical of normal operation.

## 1 INTRODUCTION

Wheel rail contact is always a hot topic for railway vehicle dynamics researchers and wheel track maintenance engineers. The knowledge of dynamic wheel rail contact stress is useful in assessing strength and fatigue life, wear of the wheel profile and rail head, and as criteria to optimize new profiles of wheel and rail.

The wheel rail stresses can be divided into surface contact stresses, subsurface stress and strain field. For a general case with elastoplastic material and arbitrary geometries and loads, finite element method(FEM) or boundary element method(BEM) is often used to get a good approximate solution[1,2]. FEM and BEM both require considerable numerical effort and this limits the applications.

Considering elastic materials of the wheel and the rail and rolling contact under vertical loading, Hertzian theory provides the normal pressure distribution and Kalker's theory gives tangential surface contact forces(creep forces) [3]. As the surface forces including normal stress and tangential creep forces can be calculated, the subsurface stress and stain field can be determined. The present paper investigates parameters affecting wheel rail contact stresses and wheel rail rolling contact creepages using simulation of dynamic wheel rail contact stresses with a complete wagon model and various track conditions.

## 2 STRESSES AT CONTACT SURFACE

When a wheel and rail are brought into contact under the action of the wheel load, the area of contact and the normal pressure distribution are usually expressed as half elliptic by Hertzian theory. For a purely normal wheel load without tangential traction, the state of stress at the surface is nearly hydrostatic on an elliptical area with semi-axes $a$ and $b$. Due to the wagon motion the effective wheel load is the sum of dynamic and static load components. The wheel load will produce wheel rail rolling contact stress on the contact area where the position of the contact area varies according to lateral and yaw displacement of wheelset.

If only the maximum stresses distribute along rolling direction($x$ axis) are considered, the two-dimensional model of an infinite cylinder subjected to normal and tangential loading is often used for simplified analysis. In the case of full sliding, the stresses at the contact surface due to both the pressure and the tangential traction can be written as [4]

$$\sigma_x = -p_0\sqrt{1-\frac{x^2}{a^2}} \pm 2\mu\frac{x}{a}, \tag{1}$$

$$\sigma_z = p_0\sqrt{1-\frac{x^2}{a^2}}, \tag{2}$$

$$\tau_{xz} = \mp\mu p_0\sqrt{1-\frac{x^2}{a^2}} \tag{3}$$

Outside the area of contact, $\sigma_z, \tau_{xz}$ are zero and the normal stress in longitudinal direction is

$$\sigma_x = \mp 2\mu p_0\left[\frac{x}{a} - sign(\frac{x}{a})\sqrt{\frac{x}{a}-1}\right] \tag{4}$$

For the state of plane strain, the normal stress in lateral direction is always

$$\sigma_y = \nu(\sigma_x + \sigma_z) \tag{5}$$

With Poisson's ratio $\nu$.

With the maximum pressure given by $p_0 = \frac{3N}{2\pi ab}$, where the $N$ is the normal load, $a$, $b$ are the semi-axis dimensions of the contact ellipse and $\mu$ is friction coefficient.

For three-dimensional elastic bodies in rolling contact without sliding friction, neglecting the effect of friction on normal pressure then the normal stress and tangential surface forces can be determined by Kalker's theory according from the calculated contact creepages and spin. Generally, these are adequate to estimate fatigue and predict wear.

## 3 FACTORS FOR AFFECTING THE WHEEL RAIL CONTACT STRESSES

For given materials of wheel and rail, and the profiles of wheel and rail, the factors affecting wheel rail contact stresses are only two: normal load $N_d$ and creepages. The former depends on vehicle system, track structure and wheel rail interaction, the creepages involve running speed and running state of the vehicle. Using a refined vehicle model will provide more accurate normal load and creepages. Modelling of the wagon will be discussed in section 4. Here we need to discuss the creepages calculation.

At present there exist several formulae to calculate lateral wheel rail contact creepages in literature. They can be divided into two families. The main terms of one can be expressed as[5,6]

$$\nu'_{yj} = (*)\cos(\gamma_j) \quad j = 1,2 \tag{6}$$

The main terms of the other can be written as[7,8,9]

$$\nu_{yj} = (*)/\cos(\gamma_j) \tag{7}$$

Where $(*)$ stands for other terms of the lateral creepage, $\nu_{yj}$. The difference between them is

$$\frac{\nu_{yj}}{\nu'_{yj}} = \frac{1}{\cos^2(\gamma_j)} \tag{8}$$

Where $j$=1 stands for right hand side wheel rail contact point and $j$=2 left hand side. The difference in lateral creepage calculated by the two different methods will increase with increase of contact angle, $\gamma$. For example, if the contact angle is $45^o$ the different is up to 2. Why does there exists the two different formulae for the determination of lateral creepage? The following analysis could be helpful.

The creepages are defined by

$$\nu_{xj} = \frac{W_{txj}}{V}, \nu_{yj} = \frac{W_{tyj}}{V}, \phi_{sj} = \frac{\Omega_{nj}}{V} \tag{9}$$

Where $W_{txj}, W_{tyj}$ stand for the relative longitudinal and lateral velocities between a wheel and rail, $\Omega_{nj}$ is relative angular velocity between a wheel and rail. $V$ is the actual velocity of the wheelset.

Selecting the origin of coordinate system at the mass centre of wheelset with the $x$ axis positive forward, $y$ axis positive to the right and $z$ axis positive downward, then the total velocity and angular velocity of a wheelset can be expressed as[7,8]

$$v_w = [V + \dot{x}_w \quad \dot{y}_w \quad \dot{z}_w]^T \tag{10}$$

and

$$\omega_{ws} = [\dot{\phi}_w + V\psi_w / r \quad \dot{\chi}_w - V/r \quad \dot{\psi}_w - V\phi_w / r]^T \tag{11}$$

Where, $\dot{x}_w, \dot{y}_w, \dot{z}_w$, sands for the velocity of the parasitic motion of wheelset in longitudinal, lateral and vertical directions, respectively. $\phi_w, \psi_w$ and $\dot{\phi}_w, \dot{\psi}_w$ are the rotational angles and rotational velocities of the wheelset in roll and yaw direction, respectively. $\dot{\chi}_w$ stands for the perturbation of the angular speed of a wheelset and $r = 2r_l r_r/(r_l + r_r)$, here we take $r = r_l = r_r$.

We suppose the track to be rigid so the rail velocity is zero at the wheel/rail contact point. Then the velocity at the contact point is

$$v_{cj} = v_w + \tilde{\omega}_w r^*_{cj} \tag{12}$$

where $\tilde{\omega}$ stands for screw symmetrical matrix:

$$\tilde{\omega}_w = \begin{bmatrix} 0 & -(\dot{\psi}_w - V\phi_w/r) & \dot{\chi}_w - V/r \\ \dot{\psi}_w - V\phi_w/r & 0 & -(\dot{\phi}_w + V\psi_w/r) \\ -(\dot{\chi}_w - V/r) & \dot{\phi}_w + V\psi_w/r & 0 \end{bmatrix} \tag{13}$$

and

$$r^*_{cj} \approx [\mp b\psi_w \quad \pm b - r\phi_w \quad \pm b\phi_w + r]^T \tag{14}$$

Neglect the high order terms and then the resulting velocity vector is

$$v_{cj} = \begin{bmatrix} \dot{x}_w + r\dot{\chi}_w \mp b\dot{\psi}_w \\ \dot{y}_w - r\dot{\phi}_w - V\psi_w \\ \dot{z}_w \pm b\dot{\phi}_w \pm bV\psi_w / r \end{bmatrix} \tag{15}$$

The components of the $v_{cj}$ project onto the contact

plane are

$$\begin{bmatrix} W_{txj} \\ W_{tyj} \\ W_{nj} \end{bmatrix} = \begin{bmatrix} 1 & 0 & 0 \\ 0 & \cos\gamma & \pm\sin\gamma \\ 0 & \pm\sin\gamma & \cos\gamma \end{bmatrix} \begin{bmatrix} \dot{x}_w + r\dot{\chi}_w \mp b\dot{\psi}_w \\ \dot{y}_w - r\dot{\phi}_w - V\psi_w \\ \dot{z}_w \pm b\dot{\phi}_w \pm bV\psi_w / r \end{bmatrix} \quad (16)$$

If high order terms are neglected then the components become

$$W_{txj} = \dot{x}_w + r\dot{\chi}_w \mp b\dot{\psi}_w \quad (17)$$

$$W_{tyj} = (\dot{y}_w - r\dot{\phi}_w - V\psi_w)\cos\gamma \pm (\dot{z}_w \pm b\dot{\phi}_w \pm bV\psi_w / r)\sin\gamma \quad (18)$$

$$W_{nj} = \pm\sin\gamma(\dot{y}_w - r\dot{\phi}_w - V\psi_w) + (\dot{z}_w \pm b\dot{\phi}_w \pm bV\psi_w / r)\cos\gamma \quad (19)$$

There are two conceptions: one considers the relative velocity in normal direction is not zero[5,6] and in that way with Eq.(9) the final creepages are

$$v_{xj} = (\dot{x}_w + r\dot{\chi}_w \mp b\dot{\psi}_w)/V \quad (20)$$

$$v_{yj} = \frac{(\dot{y}_w - r\dot{\phi}_w - V\psi_w)\cos\gamma}{V} \pm \frac{(\dot{z}_w \pm b\dot{\phi}_w \pm bV\psi_w / r)\sin\gamma}{V} \approx \frac{(\dot{y}_w - r\dot{\phi}_w - V\psi_w)\cos\gamma}{V} \quad (21)$$

The other one Eq (7) considers the normal velocity, $W_n$, is zero[7,8,9] and then the lateral creepage can be obtained below.

From $W_n$=0 from Eq. (19) yields

$$(\dot{z}_w \pm b\dot{\phi}_w \pm bV\psi_w / r) = \pm\frac{\sin\gamma}{\cos\gamma}(\dot{y}_w - r\dot{\phi}_w - V\psi_w) \quad (22)$$

Instituting the above Eq. into (18) one get

$$v_{yj} = \frac{\dot{y}_w - r\dot{\phi}_w - V\psi_w}{V\cos\gamma} \quad (23)$$

We take the symbol "+" for $j$=1 and "-" for $j$=2 in the all equations in this section.

Which one should be selected? It is noted that for the creepages calculation we assume that wheel rail contact is not separation or penetration. From this point formula (23) will be selected in our wagon model. It also acknowledged that it may be argued that the contact between wheel and rail can be modelled by a Hertzian spring and penetration is permitted.

## 4 WAGON MODEL

A wagon with three-piece bogies was selected as it is widely used in Australia. Roughly speaking, a wagon consists of 11 bodies: 1 wagon car body, 2 bolsters, 4 side frames and 4 wheelsets. Each body in space has 6 degrees of freedom so there are total 66 degrees of freedom for a wagon system. As the connection between wagon car body and two trucks is through two centre bowls, there are at least two constraints in the vertical direction. This kind of constraint also exists between side frames and adapters (wheelsets), Figure 1 gives 8 constraints in vertical direction. If these constraints are included in our wagon model the system then differential algebraic equations (DAE) must be used to describe the system [10]. As an alternative, the constraints can be replaced by spring connections with suitable stiffness as Figure 1 shown [11]. In this way the mathematical equations of the wagon system become a simple set of ordinary differential equation (ODE). This system of equations is much easier to solve. In this paper we will solve the system of ODEs

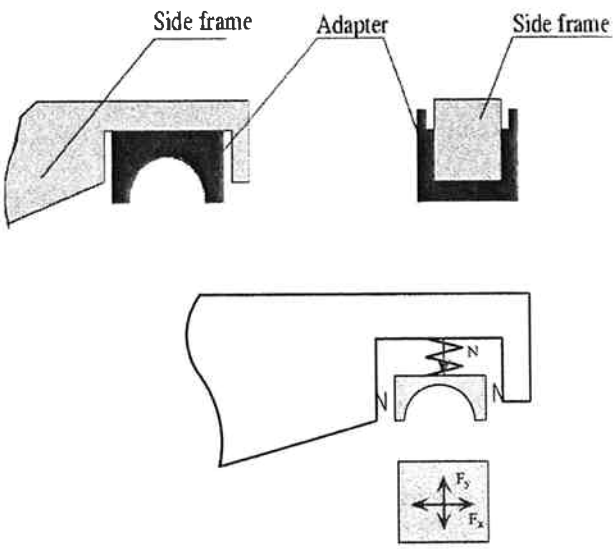


*Figure 1. Contact between side frame and adapter*

The equation of wagon system can be written as

$$[M]\ddot{X} = F_n + F_t + F_w + F_g + F_c + F_d + F_s + F_f, \quad (24)$$

The symbols in equation are below:

$M$ : System mass matrix
$F_n$ : Normal wheel rail contact force vector
$F_t$ : Tangential wheel rail contact force vector
$F_w$ : Weight vector
$F_g$ : Gyroscopic force vector
$F_c$ : Centrifugal force vector
$F_d$ : Damping force vector
$F_s$ : Spring force vector
$F_f$ : Friction force vector

To solve the system, firstly, the kinematical wheel rail contact parameters were calculated prior to simulation by the program WRKIN [8] to form the wheel rail contact table which includes the static wheel normal force as a function of the lateral and yaw of the wheelsets. The wheel rail contact parameter table is then looked-up during the simulation. The effective normal wheel force was determined by:

$$F_{nd} = \left( F_{n0}^{\frac{2}{3}} + K_h^{\frac{2}{3}} q_d \right)^{\frac{3}{2}} \tag{25}$$

Where $q_d$ is dynamic penetration, $F_{n0}$ stands for static wheel load and $K_h$ is Hertzian spring stiffness. The dimensions of the contact ellipse are then given by

$$a_d = a_0 \left[ \frac{F_{nd}}{F_{n0}} \right]^{\frac{1}{3}}, \; b_d = b_0 \left[ \frac{F_{nd}}{F_{n0}} \right]^{\frac{1}{3}}, \; a_d b_d = a_0 b_0 \left[ \frac{F_{nd}}{F_{n0}} \right]^{\frac{2}{3}} \tag{26}$$

where $a_0, b_0$ is the dimension of elliptic contact area to the static wheel load, $F_{n0}$. With the known contact dimension the tangential wheel rail contact force can be determined by Kalker theory based formulae. e.g., SHE's formulae[12].

As a three-piece bogie uses friction wedge damper system to damp out the vibration of the system, the friction phenomenon should reasonably described. Due to the lateral and vertical motion of a bolster relative to side frames the friction on the surfaces of the wedge is two-dimensional. According to friction nature, the relative motion between two contact bodies is stick-slip motion. The same case exists for the side frame contacting with adapters.

There are several ways to describe friction. In the present paper we take the method used in Vampire as a basis, to develop another suitable two-dimensional friction element[13]. The principle can be shortly expressed as (see figure 2):

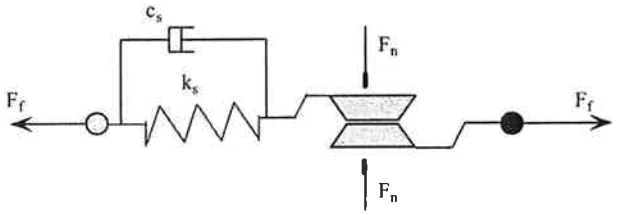


*Figure 2. Friction element used in Vampire*

$$F_f = \begin{cases} k_s \Delta d, & k_s \Delta d \le F_{fs} \;\&\; |v_r| \le \delta v_r, \\ F_{fs}, & k_s \Delta d > F_{fs} \;\&\; |v_r| \le \delta v_r, \\ F_{fk}, & |v_r| > \delta v_r. \end{cases} \tag{27}$$

Where $F_{fs} = N\mu_s sign(v_r)$ stands for static friction force; $F_{fk} = N\mu_k sign(v_r)$ is kinetic friction force; $\Delta d$ stands for resultant relative displacement and $v_r$ is relative velocity and $\delta v_r$ stands for a small value of relative velocity for numerical analysis requirement. Static and kinetic friction coefficients are represented by $\mu_s$ and $\mu_k$, respectively.

For the two-dimensional case the components of friction forces in x and y directions from Eq. (27) are:

$$F_{fx} = \begin{cases} k_s \Delta d_x, & k_s \Delta d \le F_{fs} \;\&\; |v_{rs}| \le \delta v_r, \\ F_{fs} \Delta d_x / \Delta d, & k_s \Delta d > F_{fs} \;\&\; |v_{rs}| \le \delta v_r, \\ F_{fk} v_{rx} / v_{rs}, & |v_{rs}| > \delta v_r. \end{cases} \tag{28}$$

$$F_{fy} = \begin{cases} k_s \Delta d_y, & k_s \Delta d \le F_{fs} \;\&\; |v_{rs}| \le \delta v_r, \\ F_{fs} \Delta d_y / \Delta d, & k_s \Delta d > F_{fs} \;\&\; |v_{rs}| \le \delta v_r, \\ F_{fk} v_y / v_{rs}, & |v_{rs}| > \delta v_r. \end{cases} \tag{29}$$

Where $\Delta d$, $v_{rs}$ are defined by

$$\Delta d = \sqrt{\Delta d_x^2 + \Delta d_y^2}, \quad v_{rs} = \sqrt{v_{rx}^2 + v_{ry}^2} \tag{30}$$

and for this case $F_{fs} = N\mu_s$ and $F_{fk} = N\mu_k$.

In the same way the friction torque acting on joint can be written as

$$T_f = \begin{cases} k_\beta \Delta\beta, & k_\beta \Delta\beta \le T_{fs} \;\&\; |\omega_r| \le \delta\omega_r, \\ T_{fs}, & k_\beta \Delta\beta > T_{fs} \;\&\; |\omega_r| \le \delta\omega_r, \\ T_{fk}, & |\omega_r| > \delta\omega_r. \end{cases} \tag{31}$$

Where $k_\beta$ stands for torsion spring stiffness connecting two relative rotation bodies; $\Delta\beta$ is relative rotation angle; $\omega_r$ stands for relative rotation velocity; $\delta\omega_r$ is a small value of relative rotation velocity required numerically; $T_{fs}$ stands for static friction torque and $T_{fk}$ for kinetic friction torque

The wagon model has 66 degrees of freedom and the model is implemented with C++, so we call it the C66 model.

## 5 SIMULATION RESULTS

A hopper wagon is used for this investigation. Some parameters of the wagon are listed below.

| | |
|---|---|
| Semi-spacing of truck | 5.18m |
| Half axle spacing of wheelset | 0.838 m |
| Lateral semi-spacing of primary suspension | 0.8 m |
| Wheel radius | 0.425 m |
| Semi spacing of side support | 0.616 m |
| Truck distance | 14.820 m |
| Wedge static friction coefficient | 0.4 |
| Static load on wedge friction surface | 20.0 KN |

| | |
|---|---|
| Car body mass(empty/loaded) | 8.1/66.10 Mg |
| Car body roll inertia(empty/loaded) | 10.4/85.58 $Mgm^2$ |
| Car body pitch inertia | 79.3/647.18 $Mgm^2$ |
| Car body yaw inertia | 80.0/652.98 $Mgm^2$ |
| Side frame mass | 0.447 Mg |
| Side frame roll inertia | 0.101 $Mgm^2$ |
| Side frame pitch inertia | 0.1156 $Mgm^2$ |
| Side frame yaw inertia | 0.1156 $Mgm^2$ |
| Bolster mass | 0.465 Mg |
| Bolster roll inertia | 0.175 $Mgm^2$ |
| Bolster pitch inertia | 0.115 $Mgm^2$ |
| Bolster yaw inertia | 0.176 $Mgm^2$ |
| Wheelset mass | 1.12 Mg |
| Wheelset roll and yaw inertia | 0.4201 $Mgm^2$ |
| Wheelset pitch inertia | 0.1 $Mgm^2$ |

The combination of the profiles of wheel and rail is ASLW3/AS60. In order to verify the C66 model we did comparison of the results between C66 and Vampire in many cases, Figure 3 shows the case of vertical sinusoidal track irregularity.

We use the power spectral density (PSD) formulae of FAR (Federal America Railroad) to generate track irregularity from track class 4 to class 6. For the page limitation here we only provide the results for the empty wagon on class 5 track as shown in Figures 4, and 5.

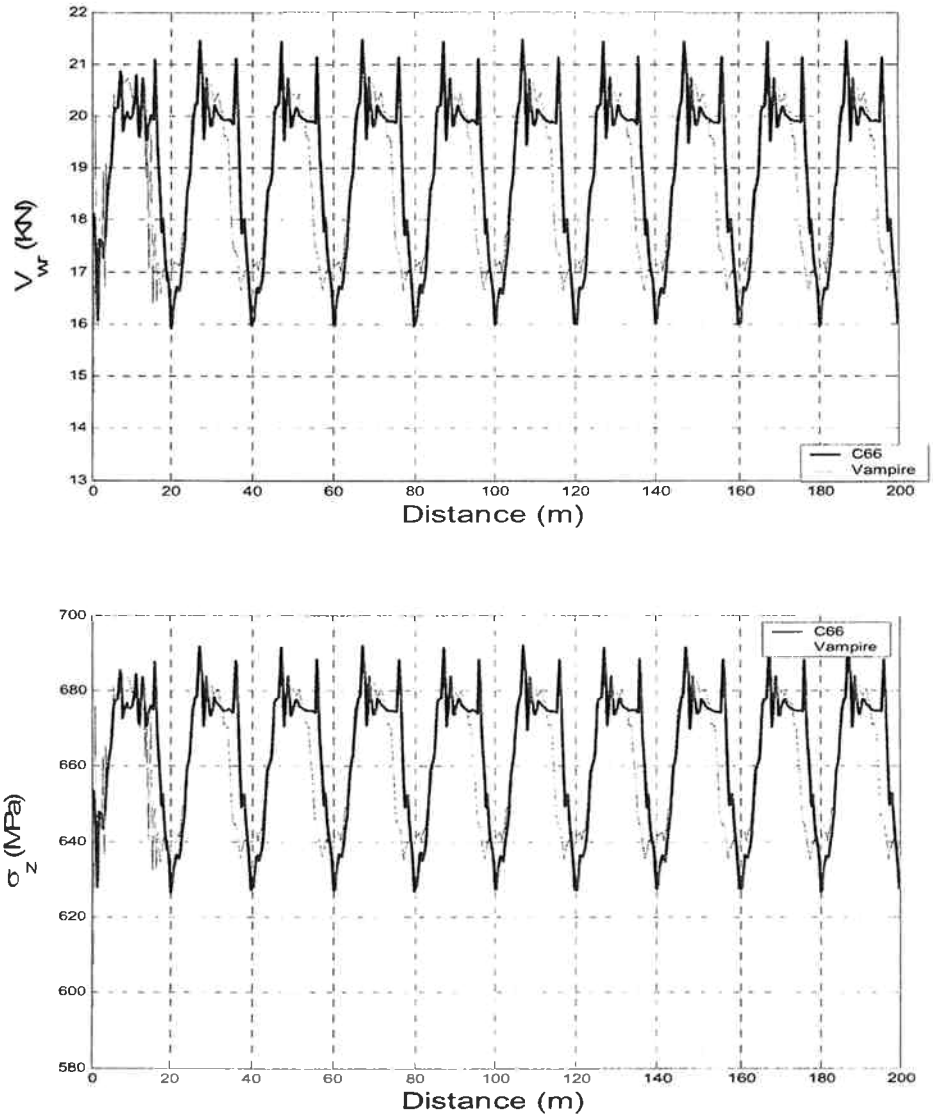


*Figure 3. Results comparison of C66 and VAMPIRE. Top: Vertical wheel rail contact force of leading wheelset. Bottom: Maximal contact stress of leading wheelset. Excitation: vertical track irregularity with* $z = 10\sin\left(\frac{2\pi s}{20}\right)$ *mm, running velocity* $V = 20m/s$. *Empty wagon is used.*

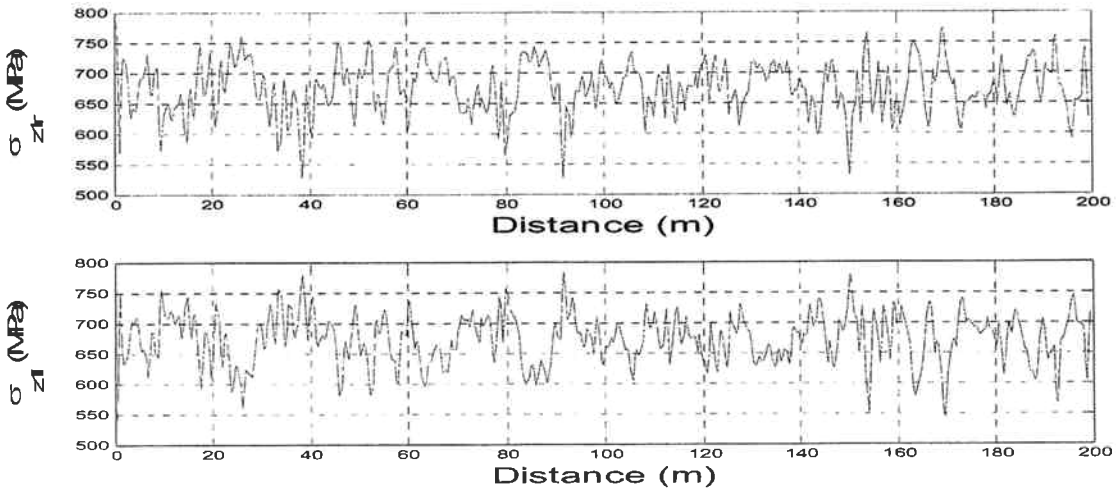


*Figure 4. Wheel rail contact stresses of leading wheelset for empty wagon on class 5 track.*

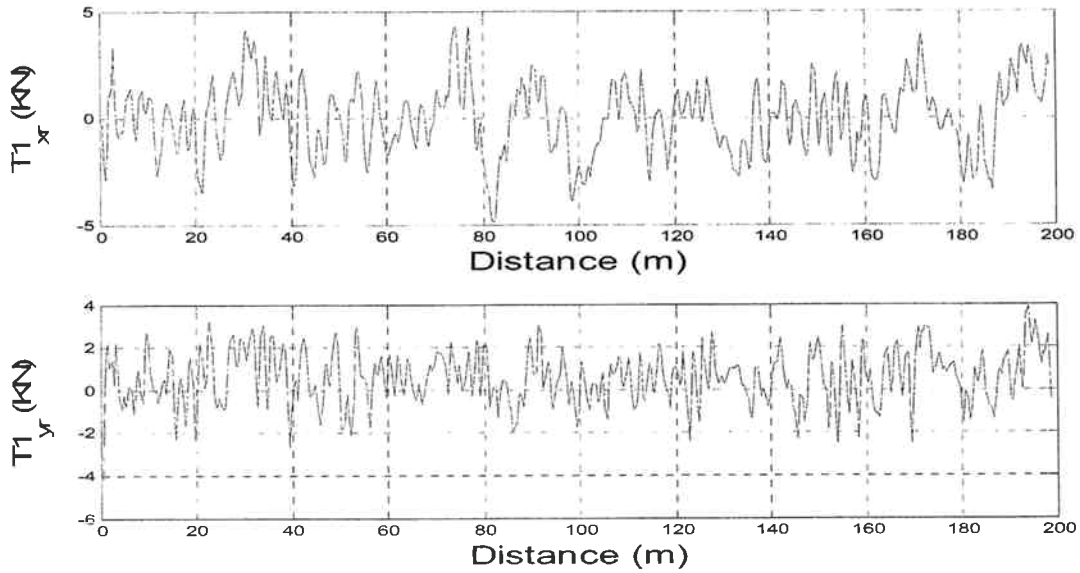


*Figure 5. RHS wheel-rail contact Creep forces of leading wheelset for empty wagon on class 5 track.*

More simulation results are shown in Table 1. As the dynamic wheel rail contact stresses vary with time, only the ranges of the minimal and maximal values are presented.

*Table 1. Simulation cases*

| No. | Track irregularity | Empty or loaded car | Speed (*m/s*) | Radius of curve (*m*) | Elevation of outside rail(*mm*) | Maximal normal stress level(*Mpa*) | Log. Creep force (*KN*) | Lateral creep force (*KN*) |
|---|---|---|---|---|---|---|---|---|
| 1 | Class6 | Empty | 20 | ∞ | 0 | 630-730 | -3--3 | -1--2 |
| 2 | Class5 | Empty | 20 | ∞ | 0 | 550-760 | -4--5 | -3--4 |
| 3 | Class4 | Empty | 16 | ∞ | 0 | 450-800 | -4--6 | -5--5 |
| 4 | Class6 | Loaded | 20 | ∞ | 0 | 1040-1095 | -7--7 | -5--5 |
| 5 | Class5 | loaded | 20 | ∞ | 0 | 1020-1120 | -11--11 | -10--10 |
| 6 | Class4 | Loaded | 20 | ∞ | 0 | 1000-1135 | -15--15 | -10--10 |
| 7 | No | Empty | 20 | 200 | 120 | 500-1000 | -1--4.5 | -0.8--4.5 |
| 8 | No | Empty | 20 | 500 | 120 | 650--665 | 0--4 | -0.8--3.8 |
| 9 | No | Empty | 20 | 1000 | 100 | 675--700 | 0--3.5 | -0.8--3.5 |
| 10 | No | Loaded | 20 | 200 | 120 | 900--1400 | -5--25 | -5--20 |
| 11 | No | Loaded | 20 | 500 | 120 | 960--1120 | -1--19 | -3--18 |
| 12 | No | Loaded | 20 | 1000 | 100 | 1020-1090 | -3--13 | 0--10 |

According to BR standard criteria for wagon the normal stress should be less than $1600Mpa$ . From the results in Table 1 all values of normal stresses are under the criteria level.

## 6 CONCLUSION

The rolling contact stresses are dependent on the wagon dynamics as illustrated by the different stress levels resulting from the wagon running on various tracks. The normal stress levels appear to be acceptable for class 4 to 6 tracks. Rougher track, for example, class 2 or 3 may result in normal stress levels being exceeded. Further investigation is planned.

Wheel rail rolling creepages play a key role to determine creep forces (tangential surface forces). It is noted that different results will be obtained depending on the choice of creepage formula. The differences in results increase with increasing wheel-rail contact angle.

A 66 DOF wagon system dynamic model was developed with a typical Australia hopper wagon to simulate wheel rail contact stresses on various tracks. The two-dimensional dry friction on the surfaces of wedges and adapters were described by a friction element which can simulate stick-slip modes.

Twelve cases for wheel rail contact stresses are simulated. The results show that the wheel rail maximal normal contact stresses of Australia wagon for the track surface irregularities simulated are under the limitation ($1600Mpa$) in all the cases.

## ACKNOWLEDGMENTS

The paper is supported by the Cooperative Research Centre for Railway Engineering and Technologies of Australia (Rail CRC) project 147. The work is also obtained support from the Centre for Railway Engineering (CRE) at Central Queensland University and Faculty of Engineering and Physical Systems, Central Queensland University.

## REFERENCES

[1] Makoto Akama, Tadao Mori, Boundary element analysis of surface initiated rolling contact fatigue cracks in wheel/rail contact systems, Wear 253(2002) pp.35-41.

[2] Massimiliao Pao at el., Distribution of contact pressure in wheel-rail contact area, Wear 253(2002),pp.256-274.

[3] J.J. Kalker, Three-Dimensional Elastic Bodies in Rolling Contact, Kluwer Academic Publishers, 1990.

[4] M.Ertz, K. Knothe, Thermal stress and shakedown in wheel/rail contact, Archive of Applied Mechanics 72(2003) 715-729.

[5] Vijay K. Garg and Rao V. Dukkipati, Dynamics of Railway Vehicle Systems, Academic Press, 1984.

[6] G. Chen and W.M. Zhai, A new wheel/rail spatially dynamic coupling model and its verification, Vehicle System Dynamics, Vol. 41,No. 2, pp.301-322.

[7] John A. Elkins, Prediction of wheel/rail interaction: the state-of-the –art, Vehicle System Dynamics(Supplement), V20, 1991.

[8] Fujie Xia, The Dynamics of the Tree-piece-freight Truck, PhD. Thesis, Informatics and Mathematical Modelling, the Technical University of Denmark, 2002.

[9] De Pater A.D., Meijers P. and Shevtsov I.Y., Simulation of the motion of a railway vehicle along curved tracks, Part I General theory, Report No. LTM 1196, Laboratory for Engineering Mechanics, Delft University of Technology, 1999.

[10] Edda Eich-Soellner, Clause Fuhrer, Numerical Methods in Multibody Dynamics, B.G. Teubner Stuttgart, 1998.

[11] AEA Technology, VAMPIRE User Manual, C2.24, Version 4.2, 2002.

[12] Z.Y. Shen, J.K.Hedrick, J.A. Elkins, A comparison of alternative creep-force models for rail vehicle dynamic analysis, Proceedings of the 8th IAVSD Symposium, MIT, Cambridge, MA, 1984.

[13] Fujie Xia, Colin Cole and Peter Wolfs, The effects of the friction between frame and adapters on the performance of three-piece truck, Proceedings of ASME/Joint Rail Conference, April 4-6, 2006, Atlanta, Georgia